1

Graphene-Based Nanomembranes for Sustainable Water Purification Applications

Uluvangada T. Uthappa[1], Dusan Losic[2,3], and Mahaveer D. Kurkuri[1]

[1] *JAIN University, Centre for Nano and Material Sciences, JAIN Global Campus, Bengaluru, Karnataka, 562112, India*
[2] *The University of Adelaide, School of Chemical Engineering, Adelaide, SA, 5005, Australia*
[3] *The University of Adelaide, ARC Research Hub for Graphene Enabled Industry Transformation, Adelaide, SA, 5005, Australia*

1.1 Introduction

The global crisis on water scarcity ranks top among the world's major problems. Provided with recent statistics, two-thirds of the world population will face major difficulties by 2025 due to the lack of water facilities. Due to the rapid population expansion, industrial development, and water pollution, it incessantly depleted freshwater resources. The extreme consumption of freshwater resources, particularly for developing countries, due to the growth of agriculture and industrial activities completely dependent on water resources and continuous utilization leads to severe ecological disasters. Thus, the shortage of water resources is an alarming issue that needs urgent resolution. To address these problems, it is crucial to conserve water resources [1].

On the other hand, membrane technology is a separation process that permeates certain species to pass via membrane while controlling the others, which is completely dependent on the properties of the membrane material. Based on their properties, membranes can be categorized as dense and porous membranes according to the driving force and ionic and molecular movement transported through membranes. Usually, it is well recognized that diverse species permeate based on the specific diffusion rates via the membranes, which are generally influenced based on solubility, diffusivity, and the membranes' porosity, as represented in Figure 1.1.

It is believed that the smaller molecules might pass through the membrane and whereas others could be blocked based on the pore sizes of the membranes. The ceramic and polymers are the most widely used membranes for water purifications plants. Typically, ceramic membranes retain better thermal and mechanical properties. However, it is difficult to control the pore size accurately with low-cost approaches. In contrast, polymeric membranes are economically and extensively utilized in microfiltration (MF), ultrafiltration (UF), nanofiltration (NF), and reverse osmosis (RO) process due to the rapid permeation and high

Environmental Applications of Carbon Nanomaterials-Based Devices, First Edition.
Edited by Shadpour Mallakpour and Chaudery M. Hussain.

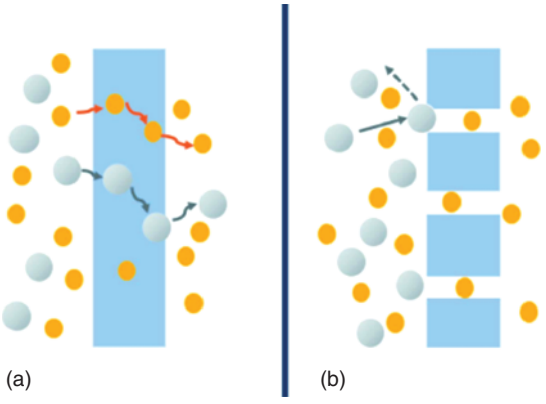

Figure 1.1 Transport mechanism for dense (a) and porous membrane (b). Source: Lyu et al. [2]. © 2018 Royal Society of Chemistry.

selectivity. However, polymers are hydrophobic that can easily adsorb target pollutants that lead to membrane fouling. Compared to ceramic and polymeric membranes, the new astonishing classic example used in membrane technology is recently discovered graphene oxide (GO). Also, reduced graphene oxide (rGO) is an important alternative class that belongs to the graphene derivative that has been explored for the development of a new generation of membrane separation technology [2]. Since from past few years' research expansion in graphene known as two-dimensional (2D) carbon allotrope and their oxidized derivatives (GO) has rapidly developed by the drastic increase in publications and patents. It is important to mention that graphene and GO have distinctive favorable material advantages compared to carbon nanotubes (CNTs) concerning separation and purification technologies. GO can be easily fabricated and engineered with favorable size, surface chemistry/modification, and structural properties. Moreover, its industrial process consumes a lesser amount of energy, making their production cost economic (for example: 500–1000 MJ/kg by solvent exfoliation of graphite or chemical reduction of GO, when compared to CNTs 100 000 MJ/kg) [3].

This chapter summarizes the very recent advances on graphene-based nanomembranes for water purifications. The properties of GO-based membranes and fabrication strategies of various graphene-based nanomembranes and their applications in desalination and dyes and some highlights on heavy metals treatment are elucidated and discussed. Finally, a conclusion and future perspectives have been provided. This current book chapter could help the researchers and experts in membrane technology working on GO-based nanomembranes for water treatment applications.

1.2 Graphene and GO-Based Membrane Characteristics and Properties

For the first time, graphene was witnessed in electron microscopes in 1962 supported on the metal surfaces. Further, it was again rediscovered in 2004 by Novoselov and Geim and awarded Nobel Prize in Physics 2010 due to their groundbreaking experiments on 2D

material graphene. Since 2010, graphene has fascinated major attractions in several applications, including water purification. Graphene contains carbon atoms bonded to each other in hexagonal patterns. The monolayered and double-layered graphene is very thin, and so it can be regarded as 2D material. Graphene's flat based honeycomb arrangements are responsible for favorable characteristic features such as strongest, lightest, most conductive, transparent materials [4], high specific surface area (2600 m^2/g), flexibility [5, 6], and large scale production from cheap raw material (graphite) [7]. GO is an oxidized form of graphene, made up of carbon atoms bonded in hexagonal honeycomb lattice structures. Based on strong oxidations surrounding environment and based on the synthetic protocol such as Hummers or Staudenmaier method, enormous groups of oxygen epoxide, hydroxyl, and carboxyl acid functional groups present in GO are represented in Figure 1.2.

Such diverse functional groups are responsible for better hydrophilicity and permit better dispersion of GO flakes in aqueous media. These substantial features significantly enable GO deposition from solution using water as an environmentally benign solvent. From the past few years, GO showed unlimited attention as a novel 2D membrane in water treatment applications due to its exceptional mechanical [8] and antifouling properties [9], atomically thin thickness, and outstanding dispersion in water [8]. Various composite membranes are obtained by mixing GO with different polymers and other surface enriched materials. Such studies have been carried to enhance surface properties such as conductivity, tensile strength, and or elasticity of materials [4]. These surface properties impart GO-based functionalized nanomembranes for advanced water treatment technologies. The selective permeation path of graphene-based membranes that allow separation via the nanopore structure originated within the basal plane of hexagonal crystalline structures.

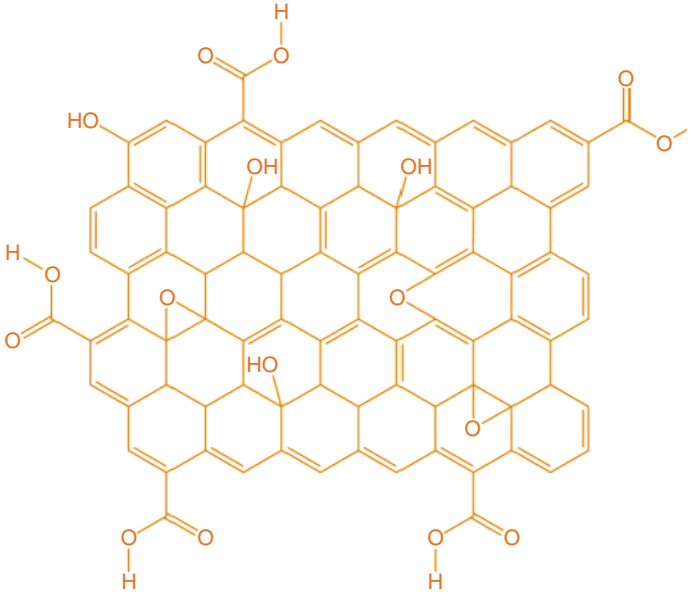

Figure 1.2 Typical chemical structure of GO showing graphene sheet derivatized by phenyl epoxide, hydroxyl groups on the basal plane, and carboxylic group on the edge.

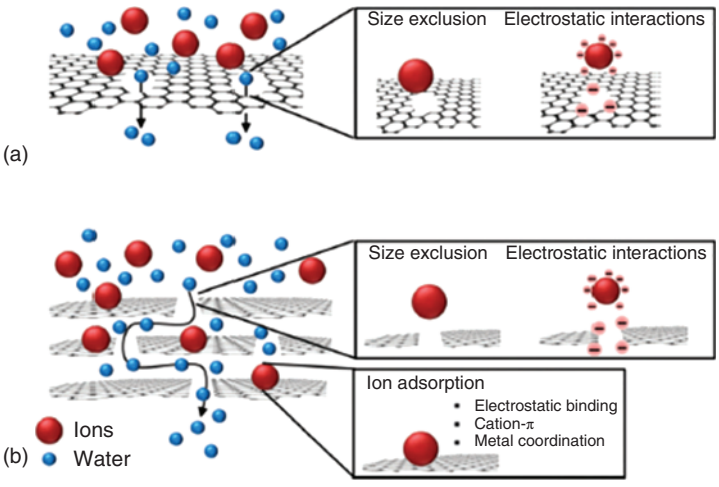

Figure 1.3 Selective permeation routes in nanoporous graphene and stacked sheets of GO. (a) Nanoporous graphene membrane and (b) stacked graphene oxide membrane. Source: Dervin et al. [9]. © 2016 Royal Society of Chemistry.

On the other hand, ions or molecules are selectively transported or passed via interlayer spacing of 2D graphene-based materials. The stacked nanosheets of GO form a multilayer laminate that shows abundant mechanical strength for application in pressure-assisted water filtration due to strong hydrogen bonds among distinct sheets. The oxygen comprising functional groups deposited haphazardly beside the edges of GO sheets, which maintain both significant interlayer spacing between and empty spaces among non-oxidized areas, constituting a network of nanocapillaries within the film. These nanochannels allow penetration of water molecules and successive transport laterally on hydrophobic non-oxidized regions of membranes that could support the rapid flow of water molecules. Thus liquid, vapors, and gases are opposed, as shown in Figure 1.3. In addition, water-soluble oxygen functional groups present beside the GO sheets, which adsorb water molecules and further diffused between the non-polar hydrocarbon present on the backbone of GO. Such permeation of water escalates the interlayer spacing in the middle of stacked GO sheets and helps in water flux over nanochannels at a higher flow rate. It has also been recognized that smaller ions enter GO membranes considerably superior to simple diffusion. Conversely, enlargement of nanochannels during the hydrated state only accepts ions of analogous sizes [9].

1.3 Fabrication of Graphene-Based Nanomembranes for Water Treatment Applications

1.3.1 Desalination

The membrane-based desalination method is classified based on membrane pore size and rejection mechanisms [10]. Desalination is a process of removing salts from seawater or

brackish water, and it is known to be the core technology for improving freshwater scarcity [11]. To improve the desalination process and enhance water treatments, innovative technological classes of membrane systems are advanced. However, to overcome the costs and energy demands accompanied by membrane treatment, advanced, innovative, and economical membranes are highly desirable [9].

1.3.2 Treatment for Dyes

Many dyes are used to color the products from various industries such as food, paints, leather, plastics, and textiles. The significant amount of effluents from those industries creates serious ecological complications to the environment for most of the underground and surface water bodies. Moreover, dye waste turbidity results in blocking sunlight and reducing diffusion into the water that could obstruct the biological process. As far as concerned, organic dyes are highly stable, toxic, carcinogenic, and mutagenic. In some cases, these properties lead to organ damage and abnormalities in living creatures. As a result, it is crucial to treat or remove such dyes before discharging them into environments [12].

1.3.3 Graphene Nanomembranes for Salt and Dye Rejection

In this report, charged nanochannels produced in polyelectrolyte intercalated amine reduced graphene oxide membranes (PE-ArGO membrane) were reported. The overall synthetic process is shown in Figure 1.4. The PE-ArGO membrane with a rejection sheet of around 160 nm in thickness with laminate structural topographies with a smooth top surface of low roughness of around 17.2 nm. The PE-ArGO membrane was *in situ* modified

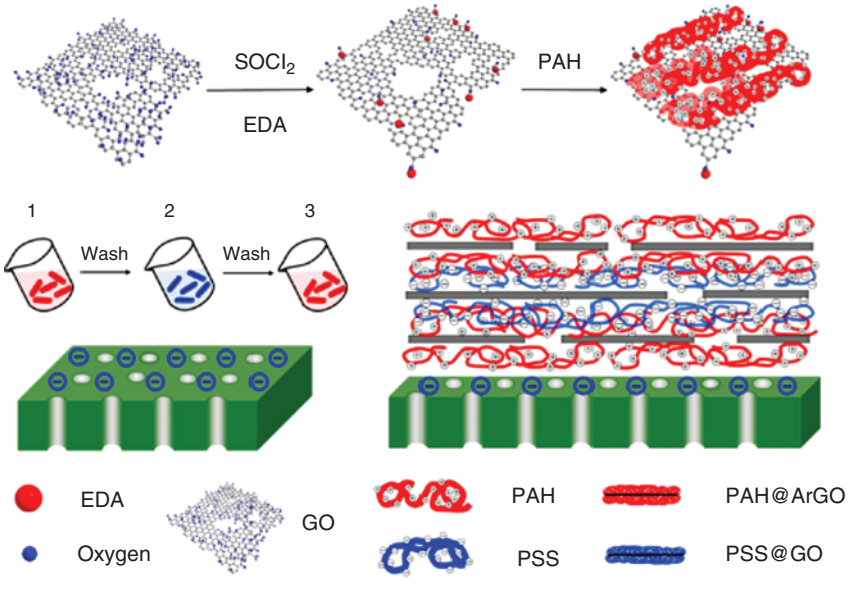

Figure 1.4 Schematic showing synthetic for PE-ArGO membrane. Source: Song et al. [13]. © 2017 American Chemical Society.

(m-PE-ArGO) using free chlorine scavenging to adjust the charge, though keeping modification to the layered structure in a nominal way. The PE-ArGO and m-PE-ArGO membrane surface charge were +4.37 and −4.28 mC/m^2. Using the pressure-assisted technique, pure water permeability for PE@ArGO and m-PE@ArGO membrane was 2.8 and 10.8 LM^2/h/bar. The salt rejection is extremely dependent on the charge density of membranes, valence of co-ions, and size of hydrated ions. The rejection of slats for positively charged PE-ArGO membrane follows in the order of: R ($MgCl_2$), 93% > R (NaCl), 88% = R ($MgSO_4$), 88% > R (Na_2SO_4), 65%, whereas R (Na_2SO_4), 90% > R (NaCl), 85% > R ($MgSO_4$), 68% > R ($MgCl_2$), 42% followed trend for negatively charged m-PE-ArGO membranes. Altogether, this is the first report on high density positive/negative charge gated ion transport behavior studies reported in GO-based membranes [13].

Stationary repulsion force and π–π contact among GO nanosheets have been tuned using interlayer functionalization and external treatment. Negatively charged congo red (CR) dye with π orbital adsorbed on the nonoxide domain of GO nanosheets, interlayers cross-linked by Ca^{2+} ions via chelating reaction. The GO–CR nanosheets π–π stacking interactions altered by thermal reduction of GO/Ca/CR membrane using the hot pressing method. The interlayer spacing of GO/Ca/CR membranes tuned from 3.20 to 5.7 Å under dry conditions is observed. In wet conditions, 7.7–11 Å. In the meantime, modified GO membranes' swelling behavior decreased compared to the bare GO bare membrane. Notably, the prepared membrane showed a permeation flux of 17 LM^2/h/bar, and the rejection for methylene blue (MB) was 99.5% [14].

Wang et al. demonstrated exfoliated hydrotalcite/graphene oxide (EHT/GO) nanosheet combined through flocculation deposition and homogeneously dispersed in polyethyleneimine (PEI) solution used as an aqueous phase for interfacial polymerization. An overview of the synthetic process is shown in Figure 1.5. The prepared hybrid membranes EHT/GO displayed improved positively charged property after integrating EHT/GO into polyamide (PA) membrane compared with pristine NF and GO incorporated NF membrane. EHT/GO exhibited a more promising transport channel of water molecules

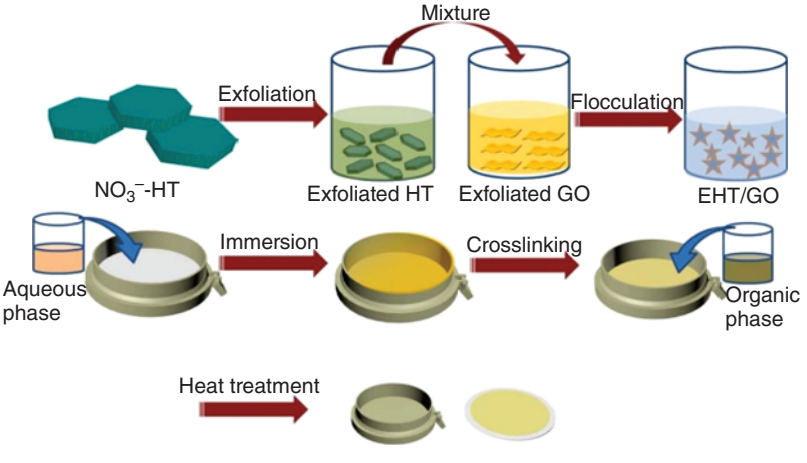

Figure 1.5 Overview of the synthetic process of EHT/GO hybrid nanosheets and nanofiltration membranes. Source: Wang et al. [15]. © 2019 Elsevier.

resulting in improved water flux of 26 LM^2/h/bar at 0.8 MPa. To this, the membrane rejection performances were 97% and 32% for 1000 ppm of Mg_2Cl_2 and Na_2SO_4 feed solutions, presenting prospective use in hard water softening applications [15].

The high rejection of organic dyes graphene oxide/attapulgite (GO/APT) composite nanofiltration membrane was developed using the vacuum-assisted filtration method. The composite membrane was fabricated by a meticulous assembly of APT nanorods incorporated into the interlayers of GO nanosheets. The APT nanorods are easily intercalated into the stacked GO lamellar layers to form stable C—O—Si bonds undergoing 3D network laminate assembly through the surface grafting functionalization. It showed a significant role in enhanced performance in water permeability. Compared with the bare GO membrane, the GO/APT membrane showed fourfold water flux performance while maintaining a high rejection rate of almost 100% for rhodamine b (RhB) dye molecules. The reason could be due to d-spacing, hydrophilicity, and 3D network lamellar structural properties. The separation mechanism was also evaluated for the GO/APT membrane with different positively/negatively charged and neutral dyes. Based on the size exclusion and electrostatic interactions, selective permeation could be done using GO/APT membranes [16]. An overview of the synthetic process is shown in Figure 1.6.

Thin-film nanocomposite (TFN) acts as an ideal platform to enhance water permeability of commercially available PA membranes in RO desalination. Thus, nitrogen-doped graphene oxide quantum dots (N-GOQD) fabricated PA/N-GOQD TFN membranes by interfacial polymerization for RO desalination applications. It is noteworthy to mention after the addition of 0.02 wt/v% N-GOQD into the PA membrane, there was a sudden enhancement of water permeability by almost three times, retaining identical salt rejection of pristine PA membrane. Improved water permeability leads to enhanced hydrophilicity of the

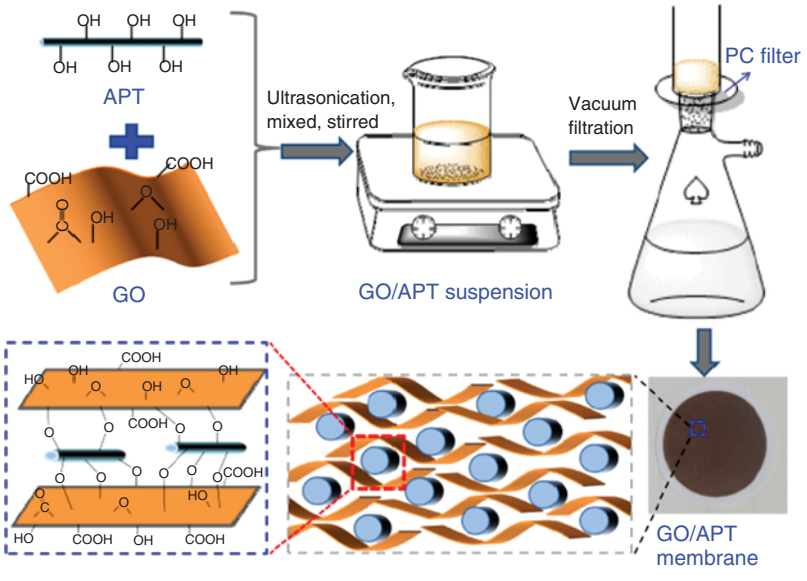

Figure 1.6 Synthetic process for GO/APT nanocomposite membrane. Source: Wang et al. [16].

membrane surface, enhanced actual membrane surface area, and a large cavity at the interface between N-GOQD and PA matrix [17].

Cheng et al. fabricated reduced graphene oxide-gold nanoparticle (rGO-AuNP) membrane by vacuum filtration for wastewater dye treatment applications. Using the TEM technique, the size of AuNPs on the rGO surface measured about 8–10 nm in size. The layer by layer (LBL) stacking of rGO-AuNP showed a high flux of 204 LM^2/h/bar and retention of 99% for RhB dye molecules [18].

GO membranes are recognized as potential candidates in separation technology. Nonetheless, their instability in aqueous environments is the drawback in real-time applications. Ma et al. designed facile eco-friendly intercalation of montmorillonite (MMT) nano patches on GO to form stable membranes, addressing such complications. The developed stable membranes showed a high water flux of 139.5 LM^2/h/bar under 0.01 MPa. Further, for various organic dye molecules such as congo red (CR), RhB, crystal violet (CV), methylene blue (MB) showed 98.75%, 99.44%, 99.90%, and 99.94% respectively [19].

In this study, carboxylation of GO nanosheets was carried out through a series of multiple oxidation methods and nucleophilic substitution reactions. Graphene acidic (GA) membrane fabricated using carboxylation of GO nanosheets through the multiple oxidation process. The developed GA membranes showed high water permeability and enhanced salt rejections when associated with bare GO and modified GO membranes with surface negative charge and hydrophilicity. GA membrane showed pure water flux of 73.5 LM^2/h/bar and peak rejection of 64% and 95% for 2000 mg/l NaCl and Na_2SO_4 feed solutions at 1.5 MPa [20].

In an aqueous solution in the absence of organic solvents GO, rGO, and graphene oxide/polyacrylamide (GO/PAM), nanofiltration membranes are prepared using vacuum filtration. The hydrophilicity of such developed graphene-based membranes was analyzed using contact angle measurements by using X-ray diffraction interlayer spacing of various membranes such as GO (0.85 nm), GO/PAM (0.68 nm), and rGO (0.36 nm). The performance studies of all these graphene-based membranes were carried out using dead-end filtration mode. The water flux and retention for RhB dye showed 399 LM^2/h/bar, 85% for GO and 188.89 LM^2/h/bar, 95.43% for GO/PAM and 85.85 LM^2/h/bar, 97% for rGO membranes. The GO/PAM membranes showed the best separation performance due to the actual fine-tuning of interlayer spacing. These could be potential membranes for high performance in water purification applications [21].

To address global water issues, forward osmosis (FO) based water treatment showed an immense impact. However, it has some limitations in practical application, like the lack of FO membranes with high permeability and selectivity. The novel reduced GO/CNT hollow fiber through electrophoretic deposition coupling with chemical reduction process with high FO performances was evaluated. Two main factors were noted. One is due to the ultralow friction, and distinct interlayer spacing of rGO showed higher water permeability and selectivity. The second factor is high porosity, and improved wettability warranted the CNT hollow fiber with low internal concentration polarization ensured and enhanced water flux. Using deionized water feed at a 0.5 M NaCl draw solution (DS), reduced GO/CNT showed exceptional water flux of 22.6 LMH, indicating 3.3 times greater than the commercial membrane. In the meantime, its reverse salt flux displayed only 1.6 gMH compared to 2.2 gMH for commercial membrane. The obtained results suggest that the rGO/CNT membrane could be a substituent for clean water supply in the FO process [22].

Cellulose acetate (CA)/GO nanocomposites were fabricated for seawater desalination using the phase inversion method. GO nanosheets with grain size 2.7 nm were added to the CA matrix and casting CA/GO onto polyester fabric to enact asymmetric CA (RO) membranes to enhance thermal and mechanical stability. Further, the addition of GO into the CA matrix altered the porosity structure. Meanwhile, synthetic seawater rejection of CA membrane modified with 1 wt% GO showed almost 90% (80% more salt rejection of bare CA membrane) for 25 000 ppm NaCl at 25 bar, which is 1.8 more when compared to bare CA membrane. Also, the flux of the CA membrane showed minor reduction (30% decrease) in the presence of 1 wt% GO showing prospective in seawater desalination [23].

Kang et al. developed graphene oxide-oxidized carbon nanotubes-layer by layer assembly (GO-OCNTs-LBL) with different bilayers on polyethersulfone (PES) membranes. The insertion of OCNTs on the GO interlayer for GO-OCNTs-LBL membrane controls the enlargement of GO. Few other studies were inspected using various salts such as NaCl, $MgCl_2$, Na_2SO_4, sucrose as DSs, and deionized water as feed. GO-OCNTs-LBL membranes showed high water flux than GO-LBL (control) for NaCl, $MgCl_2$, Na_2SO_4, and sucrose as DS. The solute flux of GO-OCNTs-LBL membrane for NaCl decreased by 70% than that of GO-LBL membrane. Consequently, the GO-OCNTs-LBL membrane showed superior rejection performances for NaCl than the GO-LBL membrane alone [24].

A polydopamine (PDA) functionalized reduced graphene oxide-metal organic frameworks (rGO-MOFs-HKUST-1) nanocomposites were developed with expeditious rejection capacity for organic dye. In this work, MOFs-HKUST-1 based on rGO was functionalized with PDA. These PDA-rGO-MOFs-HKUST-1 nanocomposites formed on the surface of commercially available CA membrane. The addition of HKUST-1 and cross-linking functionalization of PDA showed excellent rejection, flux, hydrophilic, and antifouling performances. The prepared nanocomposite membrane (PDA-rGO-MOFs-HKUST-1) could successfully reject methylene blue (99.8%) and congo red (CR) 89% efficiently. Further, it is important to note that the flux of the PDA-rGO-MOFs-HKUST-1 membrane showed a drastic increase of 31-fold due to HKUST-1 and PDA [25]. The schematic showing mechanisms involved in PDA-rGO-MOFs-HKUST nanocomposites shown in Figure 1.7.

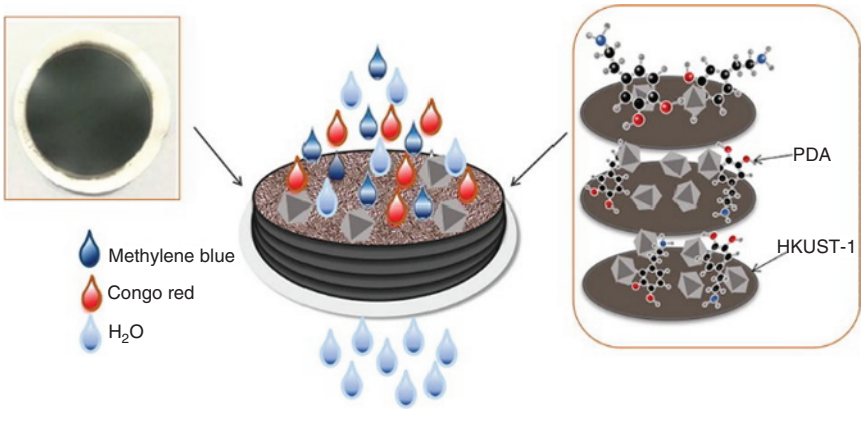

Figure 1.7 Schematic showing mechanisms involved in PDA-rGO-MOFs-HKUST nanocomposites. Source: Liu et al. [25]. © 2019 Elsevier.

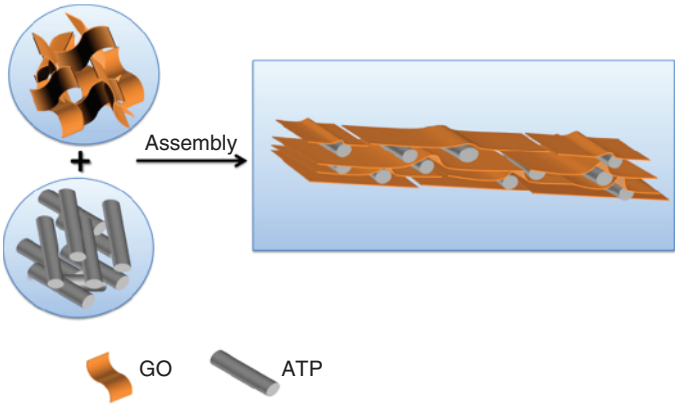

Figure 1.8 Schematic self-assembly of GO/ATP membranes. Source: Luo et al. [26]. © 2019 Elsevier.

Lee et al. effectively surface-functionalized EDTA-rGO membranes for nanofiltration. The EDTA-rGO membranes' surface was eventually treated with oxygen plasma to boost its water permeability and denoted (P-EDTA-rGO). The P-EDTA-rGO showed 80% of rejection for NaCl salt and water permeance of 150 LM^2/h/bar, showing 15 times greater than before plasma surface treatment. The developed P-EDTA-rGO nanofiltration membrane caused high rejection rates. Permeabilities of the small interlayer spacing (5.7 Å) is due to EDTA functionalization and improved hydrophilicity from enhanced plasma treatment [25].

In this work, the attapulgite (ATP) nanofibers/GO composite membrane is self-assembled by mixed solutions containing both ATP and GO shown in Figure 1.8. ATP nanofibers intercalated on GO nanosheets interlayers, acting as laminate structures for effectual trails for water molecules GO. Besides, ATP nanofibers able to widen mass transfer channels and able to promote hydration capacity. The permeate flux from 28.64 LM^2/h/bar for GO membranes (control) to 221 LM^2/h/bar for ATP/GO membranes was observed and showed extraordinary rejection rates for organic dye molecules such as CBB R250 99.88% and 99.93% for TMPyP [26].

In membrane studies, particularly in water treatment, stability is one of the major problems. In this work, Fang et al. constructed a highly water stable GO-based metal-organic framework (MOF) (UiO66) composite membrane was designed. The construction of substrate involves two main steps: (i) doping GO nanosheets into the membrane casting solution comprising polyacrylonitrile (PAN) that forms 2D–3D inter-connecting pores by phase inversion mode designated as GO-PAN, and (ii) immersing GO-PAN into dopamine solution, which undergoes self-polymerization undergoes to form better compatible and flexible substrate denoted as PGP. The UiO66 layer was assembled by vacuum-assisted filtration technique on porous PGP support illustrated in Figure 1.9. The stable GO-based UiO66/PAN, known as thin-film composite membrane, showed higher water flux 31.33 LM^2/h/bar and maintaining an effective rejection rate of >94% for various dyes such as congo red, methyl orange (MO), methylene blue, and RhB [27].

In other work, the graphene oxide framework (GOF) was designed via "from" and "to" cross-linking approaches. GOF with compact nanochannels were fabricated by LBL using branched polyethyleneimine (BPEI), GO, and thiourea particles as the well-defined

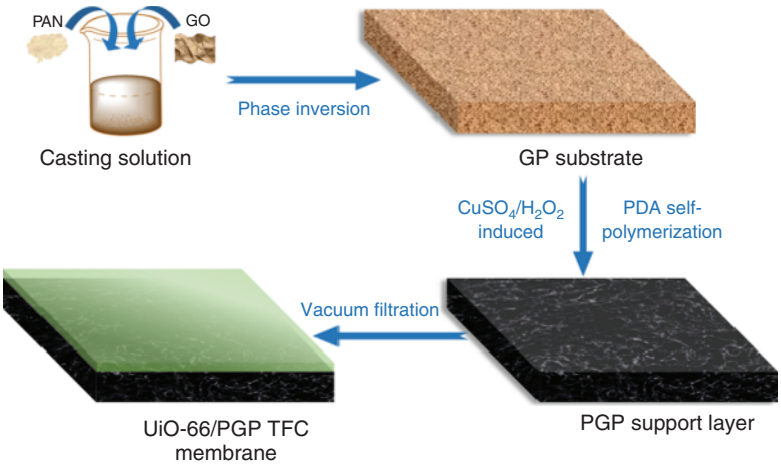

Figure 1.9 Overview process involved in the UiO66/PGP-TFC NF membrane process. Source: Fang et al. [27]. © 2020 Elsevier.

building blocks. The surface morphology of BPEI/GO/thiourea membranes revealed with compact GOF arrangement with very narrow interlamellar spacing (0.49 nm) when matched to BPEI/GO membranes (0.52 nm). Structural interpretation revealed thiourea partially reduced GO molecules mediated as "to" cross-linker linking adjacent GO nanosheets. While the GO deposition BPEI accomplished as "from" cross-linker by binding thiourea linked GO laminates to form highly stable membranes. The GOF membrane performances showed rejection of 99.5% for both anionic and cationic dyes like methyl orange and RhB. The BPEI/GO/thiourea membrane synthesized with 12 bilayers using 0.25 mg/ml of GO concentrations showed pure water flux of 24 LM^2/h/bar and Na_2SO_4 rejection of 94%, showing permeability 2.5 times when compared with commercially available nanofiltration membrane. More importantly, BPEI/GO/thiourea showed excellent stability in both acid and basic aqueous solutions [28].

A 3D graphene oxide hydrogel membranes (GOHMs) designed by gelation of GO with ferrous ions through vacuum aided filtration and their application shown in Figure 1.10. In this work, ferrous ions assisted as cross-linkers, which enhanced bonding strength between

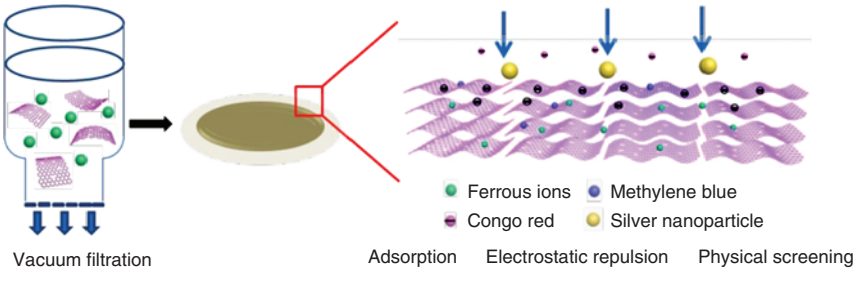

Figure 1.10 Schematic of GOHMs membrane preparation and retention mechanisms of target pollutants. Source: Chen et al. [29]. © 2019 Royal Society of Chemistry.

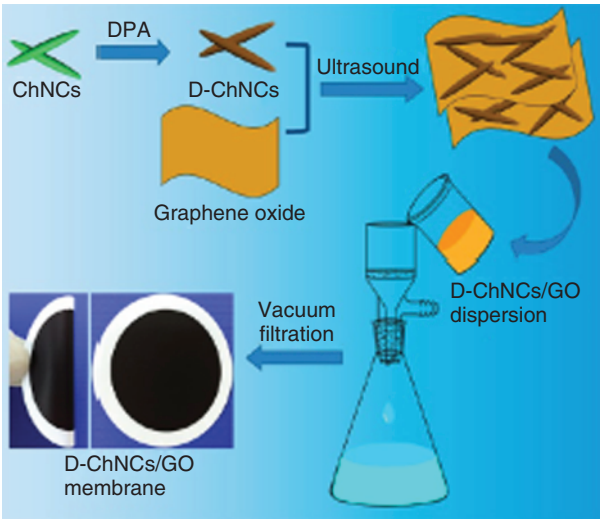

Figure 1.11 Schematic illustration of D-ChNCs and D-ChNCs/GO composite membranes. Source: Ou et al. [30]. © 2019 American Chemical Society.

GO nanosheets to prompt microstructure formation of GO via cation π interactions to form 3D lamellar porous structures. In contrast, with pristine GO membranes, the GOHMs exhibited superior water stability and enhanced water permeability of 111 LM^2/h/bar and retention performances of >99% for methylene blue and congo red dyes [29].

In this work, free-standing chitin nanocrystals (ChNCs) was modified by dopamine (D) to form GO composites and labeled as D-ChNCs-GO, and their schematic is shown in Figure 1.11. The hydrophilicity is purely based on the contents of D-ChNCs that displays a very sharp increase in water flux from 8.8 for bare GO to 135.6 LM^2/h/bar for D-ChNCs-GO composite membranes. Additionally, the rejection rates for methylene blue and congo red dye showed 99.3% and 98.3% of removal performances [30].

Januario et al. modified the PES microfiltration membrane with sulfuric acid, titanium dioxide (TiO_2), and GO solutions using the LBL self-assembly method through an electrostatic interactions pressure-driven filtration system. The separation performances of the designed membrane for various charged dye molecules were twilight yellow (TY) (69.98%), red bordeaux (BR) (93%), and safranin orange (SO) (100%) based on several factors such as size exclusion, electrostatic repulsion, and adsorptive processes [31].

The graphene oxide/MIL-88A(Fe) (GO/M88A) membrane was fabricated using the vacuum filtration method. The intercalation of M88A on graphene nanosheets showed enhanced separation performances. The designed membrane was utilized for the photo-Fenton degradation process showing 99.81% separation efficiency for methylene blue (MB) dye with enhanced 26.3 LM^2/h/bar of flux rate [32].

In this report, a nominal strategy was adapted to design graphene oxide-methylene blue (GO/MB) membrane composites. GO was surface modified by MB through electrostatic interactions and π–π conjugation systems. The rejection study for GO/MB membrane for various dyes (methyl orange, disperse black9, and RhB showed 93%, 99.85%, and 82.56% of rejections, and pure water flux was 7.67 LM^2/h/bar [33].

The GO with the 2D lamellar arrangement and single-atom thickness showed several benefits in water treatment applications assembled with the continuous membrane. Nevertheless, a suitable process to advance the improved separation property of GO membrane is highly imperative. Also, damage to the membrane during the large-scale application route, which results in a significant loss, are the main drawbacks that to be addressed. In this work, a hierarchically self-assembled GO hybrid membrane was designed to achieve superior efficiency in the water purification process and self-healing property, which leads to the synergetic effect of MOF and hydrophilic coating of chitosan biopolymer.

Intercalated MOF effectually extended the available channel space of GO and capable of molecule sieving properties. In the meantime, the chitosan-coated layer could particularly adsorb water molecules and attain self-healing via cross-linking reaction. Developed GO hybrid membrane showed enhanced water flux 14.62 LM^2/h/bar, showing an effective 344% improvement when compared with water flux of GO alone. Meanwhile, the GO hybrid membrane was able to show a rejection rate of >99% for methylene blue (MB), methyl orange (MO), acid orange (AO), and direct red 80 (DR) dyes. The damaged GO hybrid membranes can also recover their original water purification 95% for water flux and 99% of rejection ratios [34]. The schematic process of MOF–GO–CS composite membranes used for the water purification process is shown in Figure 1.12.

Due to the extraordinary permeance of GO, it has an inherent application in membrane separation. Fang et al. designed rGO by green hydrothermal reduction method. Further, the rGO membrane was synthesized on polyvinylidene fluoride (PVDF) supporting membranes by vacuum-assisted filtration. At this point, the interlayer structure of GO and the permeability of rGO membranes can be fine-tuned by altering the reduction degree of GO via altering the hydrothermal reaction time. Due to the defects of rGO nanosheets, less oxygen-bearing functional groups and improved hydrophobicity enable transport of water molecular in relatively smaller interlayer space due to hydrothermal reduction. In contrast, with the bare GO membrane, the hydrothermal reduced rGO membrane revealed excellent permeability with a rejection ratio of 99% for methyl blue, congo red, and crystal violet dyes [35].

Li et al. have designed polysulfone grafted graphene oxide nanosheets (GO-*g*-PSf) through nucleophilic substitution reaction between hydroxyl groups present in GO and chloromethyl groups of chloromethylated polysulfone (CMPSf). The GO-*g*-PSf dispersion in *N*-methyl pyrrolidone (NMP) is used to produce via vacuum filtration using PA

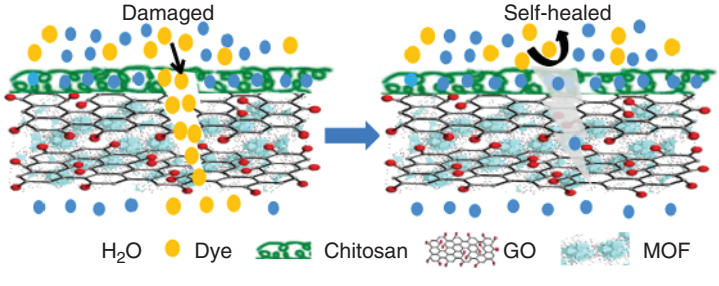

Figure 1.12 Schematic process of MOF-GO-CS composite membranes used for water purification process. Source: Chang et al. [34]. © 2019 American Chemical Society.

composite membrane as supports. GO-*g*-PSf hybrid membrane with a deposition rate of 31.8 μg/cm^2 showed superior water flux of 88 LM^2/h than pristine GO composite membrane 12.8 LM^2/h at 2 bar the enlarged interlayer spacing among the developed GO-*g*-PSf nanosheets. The rejection rate of GO-*g*-PSf membranes displayed 90% for acid black 1, 99.5% for congo red, and 99.8% for methylene blue dyes under cross-flow process at 2 bar. Notably, the water permeance of GO-*g*-PSf membrane endured at 25.9 LM^2/h after 60 hours of operation process for congo red separation. It is also worth noting that GO-*g*-PSf membrane showed enhanced structural stability after two hours of ultrasonic irradiation due to the physical enlargement of PSf chains [36]. The preparation strategies involved for GO-*g*-PSf and their chemical reaction showed in Figure 1.13.

A covalent organic framework-1 (COF-1) with systematically arranged structure and controlled pore size was covalently functionalized on the GO surface through *in situ* mode and schematically shown in Figure 1.14. The fabricated GO/COF-1 nanocomposites enhanced the dispersivity and stability in water over COF-1, permitting GO/COF-1 nanocomposites in water purification applications. The nanocomposites assembled on the PAN support to form ultrafiltration nanomembranes through dead-end filtration mode. The enhanced water permeation of 310 LM^2/h and high rejection rates for various dyes such as congo red, direct red 23, and methylene blue showing >99% of rejection rate and superior permeability for ion salts, were observed [37].

A nano graphene oxide particles (NGO), by the aid of multi-scale arrangement, were designed. In this work, divalent metal cations (Ca^{2+}, Cu^{2+}, and Mg^{2+}) engaged as cross-linking agents in order to stack nano NGO particles on both surface and pore channels of

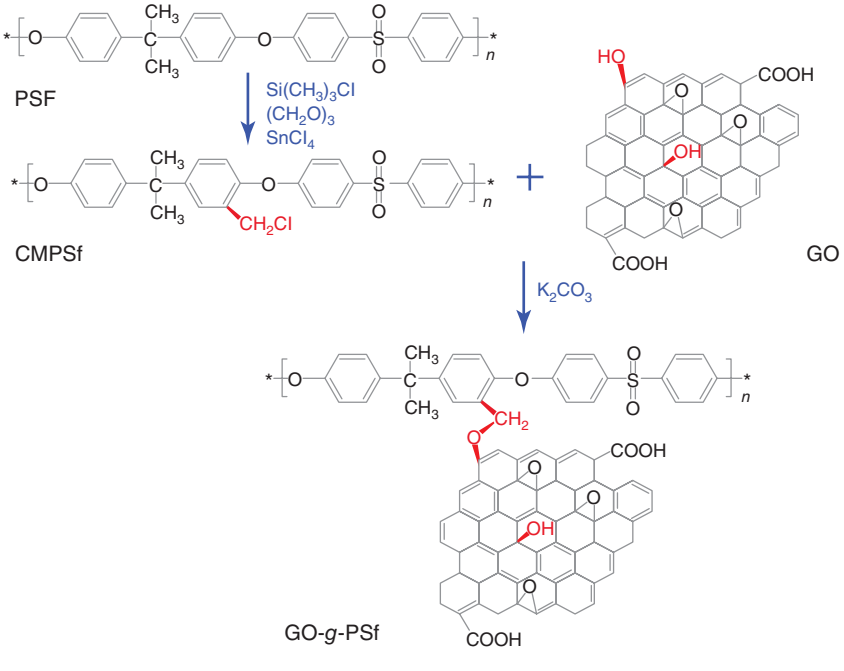

Figure 1.13 Preparation strategies involved for GO-*g*-PSf. Source: Li et al. [36]. © 2020 Elsevier.

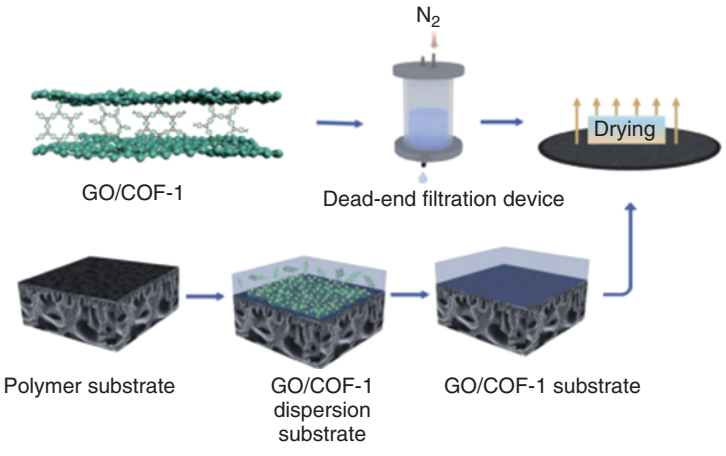

Figure 1.14 Schematic overview of GO/COF-1 membrane fabrication. Source: Zhang et al. [37]. © 2019 Elsevier.

poly(*p*-phenylene sulfide) (PPS) formed over electrostatic and coordination bonds. Metal NGO frameworks presented identical MOFs structure with nanoscale openings, and Metal-NGO/PSS membranes displayed outstanding water permeability and superior dye rejections. Compared with the transversal interlayer molecular transport chamber present in existing GO membranes, Metal-NGO/PSS membranes exhibited condensed permeable channel, maximum pore opening attaining designed membrane with rapid water molecular transport rate and superior pure water flux of 3109 LMH/MPa. Also, the Metal-NGO/PSS membranes showed a high rejection rate >98% for various dyes [38].

In another work, hybrid nanosheets were obtained by grafting GO and covalent organic frameworks (COFs) and organized building blocks. The covalent triazine framework (CTF) COFs exfoliated into nanosheets and reacted with GO to form GO-CTF hybrid nanosheets. The addition of CTF helps to change the interlayer distance between GO-CTF nanomembranes exhibiting high rejection for organic dyes >90%. Additionally, GO-CTF membranes showed a water flux of 226 LM^2/h, which is more than 12-fold higher than pristine GO membranes. Besides, chemical bonds between GO and COFs showed enhanced stability [39].

Multifunctional thin-film nanocomposites (MTFNs) nanofiltration membrane is designed using the combination of rGO@TiO_2@Ag into the PA layer was developed. The definite features of the graphene-based nanocomposites were obtained by microwave irradiation process, which recommended water channelization and provided with super hydrophilicity features. The MTFN-rGO@TiO_2@Ag preparation process is shown in Figure 1.15. Moreover, high permeability of 52 LM^2/h, desalination performances of 96% for 1 g/l Na_2SO_4 feed solution, and dye rejection of 98% for rose bengal dye feed solution of 0.5 g/l were observed [40].

In other work, unique, low-pressure nanofiltration membranes (LMPs) consisting of MoS_2 nano-supporting spacer among the GO layers are synthesized by pressure-driven assembly and heat treatment. The GO/MoS_2 showed pure water permeability of 10 LM^2/h at low pressure (2 bar), having greater than 13.6 times more when compared to pristine GO

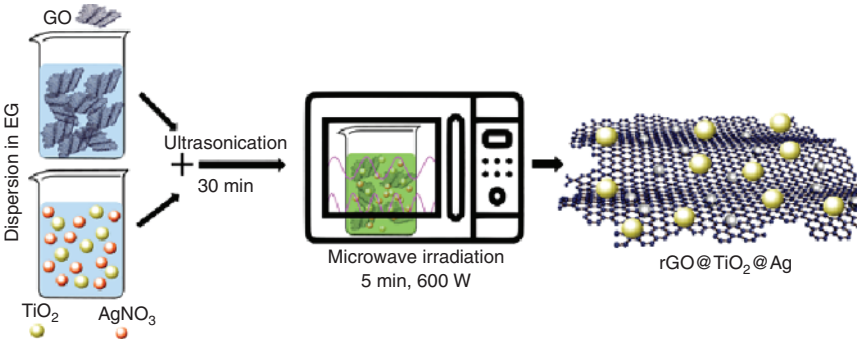

Figure 1.15 Schematic showing fabrication of rGO-TiO_2-Ag nanocomposites through microwave irradiation. Source: Abadikhah et al. [40]. © 2019 American Chemical Society.

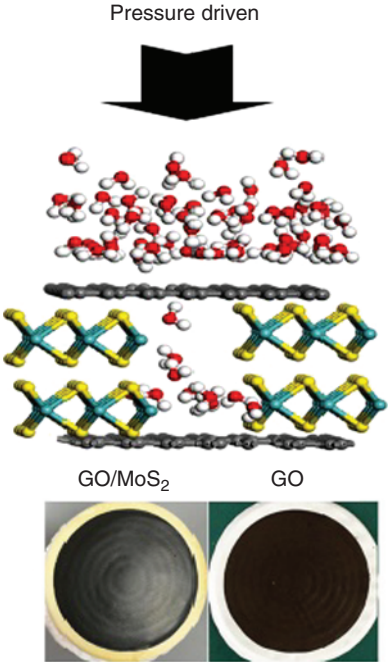

Figure 1.16 Schematic showing fabrication of GO and GO/MoS_2. Source: Zhang et al. [41]. © 2019 Elsevier.

membrane 0.75 LM^2/h. Also, high rejection for different charged dyes >95% was observed. Also, moderate salt rejections of 43%, 65%, 26.5%, and 23% for NaCl, Na_2SO_4, $MgCl_2$, and $MgSO_4$ respectively [41]. The formation of GO and GO/MoS_2 are shown in Figure 1.16.

It is well-known that the structural instability and flux deterioration factors hinder the real-time application of GO-based membranes. Thus, an innovative GO/DTiO_2-PDA-PEI dopamine modified TiO_2 hybrid nanofiltration membrane was obtained through multi couple strategy, self-assembly, co-polymerization, and surface grafting method. Fine-tuning the nanoscale interspace among the GO nanosheets and fabricating the membrane

with a positively charged surface and negatively charged subsurface with a pore size of 0.87 nm was developed. The designed membranes showed water permeance of 41.675 LM^2/h. The rejection rate for the high molecular weight of positively charged crystal violet dye 99.9%, positively charged safranine 96%, negatively charged EBT 99.9%, and low molecular weight of negative dye Alizarin yellow GG 89.4% of less performance was observed [42].

Yang et al. designed a novel nanofiltration membrane via rapid co-deposition of metal phenolic networks (MPNs) and piperazine (PIP) on a porous substrate of trimesoyl chloride using a cross-linking approach. Motivated by the catechol chemistry, tannic acid surface modified to tether PIP monomers are formed by co-deposition through coordination bonds with Fe^{3+} ions on the substrate to form Fe^{3+}/TA-PIP complex. The designed membrane showed improved water permeability of 13.73 LM^2/h and 89.52% of $MgSO_4$ rejection. Furthermore, to enhance the membrane performance, modified GO nanosheets were embedded on Fe^{3+}/TA-PIP complex, exhibiting improved water permeability of 21.66 LM^2/h and $MgSO_4$ rejection of 91% [43].

Another work revealed polyethersulfone micro-filtration membranes (mPES) functionalized with polyethilenimine and GO by LBL assembly approach through electrostatic interactions pressure-driven filtration system. The highly positively charged polyethilenimine allows easy to assemble on PES substrate to accept negative layers of GO. Finally, the designed combinations of GO/PEI showed the best performance for Blue Corazol (BC) with dye rejection of 97.8% and pure water permeability of 99.4 LM^2/h. Also, the membrane showed a flux recovery of >80% after hydraulically cleaning. Also, rejection of BC dye in real dye bath wastewater showed outstanding performance with >96% of rejection rate was observed [44].

In other reported work, ultra-thin GO films with better salt rejection made-up through contra-diffusion-induced cross-linking constructed on cation-π and electrostatic interactions between cations and GO flakes. Moreover, it is a rapid process. Only five minutes is required to design a defect-free GO film. Several cations such as Na^+, K^+, Mg^{2+}, Ca^{2+}, and Fe^{3+} are used as "cross-linkers" to design GO membranes with high separation performances. The designed membranes showed a 90% rejection for Na_2SO_4 salts with a permeance of 4.3 LM^2/h/bar [45].

In this report, UV reduced graphene oxide (UrGO) membranes supported on PVDF was designed for wastewater treatment applications. The weak reduction GO membrane showed optimal performances for removing pollutants. Due to the weak reduction of GO membrane, pristine graphitic sp^2 domains increased with a minor decrease in d-spacing. Therefore, UrGO membranes revealed a high water flux of 38.27 LM^2/h/bar by enhanced flux more than 270% compared to GO membrane alone. Also, the rejection rate of 99% was observed for RhB dye, and for other dyes such as EBT, methylene blue, crystal violet showed >96% of rejection performances [46].

To sieve small inorganic salt ions number of reports are projected by reducing the interlayer spacing down to several angstroms. On the other hand, the major challenge for such compacted graphene oxide membranes (GOMs) is a very low water flux of <0.1 LM^2/h/bar that hinders real-world applications. Planar heterogeneous graphene oxide membranes (PHGOM) with definite salt rejection and high water flux is reported. A horizontal ion transport via oppositely charged GO multi-layer heterojunction showed bi-unipolar

transport performance by blocking the conduction of both cations and anions. Furthermore, supported by the forward electric field, salt concentrations are depleted in the neutral transition area of PHGOM. In this condition, deionized water is extracted from the depletion zone. Further, undergoing all these mechanisms high rejection rate for NaCl and water flux of 1529 LM^2/h/bar was observed [47].

In other work, starch modified GO was added to the polypiperazinamide network to give superior flux hyper-branched starch functionalized graphene oxide composites (HGOST) nanofiltration membranes. The modified GO starch composites are embedded in the PA top layer by esterification. The membranes are negatively charged with the top layer and showed high rejection with 96% for Na_2SO_4 salts and pure water flux of 10 LM^2/h/bar [48].

Wang et al. proposed new multiple tailored assembly ethylenediamine cross-linked GO nanocomposites membrane on a macroporous tubular ceramic substrate. In this work, the GO nanosheets are well orderly stacked, showing the construction of efficient nanochannels for mass transfer. The subsequent membrane showed permeance of 375.75 LM^2/h/bar, which is 5.62 times superior to GO membranes, and rejection of 98.6% for EBT dye. The flux for Na_2SO_4 salt was 232.72 LM^2/h/bar, and a 78% rejection rate was observed [49].

Nonetheless, effectual tuning of rGO laminar arrangements for improved membrane performance remains a challenging task. In this work, novel 1-D graphitic carbon nitride nanotubes (g-C3N4-NTs) intercalated rGO nanofiltration (NF) membrane with the better photo-induced self-cleaning property. The g-C_3N_4-NT enlarged the rGO interlayer spacing for enhanced water permeability and has visible light photocatalytic properties to remove dye pollutants. The g-C_3N_4-NT/rGO membranes exhibited water permeability of 4.87 LM^2/h/bar and RhB removal rate of >98% for long term operation [50].

It is known that rGO membranes with narrow channels display salt rejection compared to conventional nanofiltration (NF) membranes. However, their water permeance is less due to the high tortuosity of water permeation. This report includes a simple approach to creating in-plane nanopores on the GO sheets before reduction, decreasing the tortuosity, increasing water permeance, and maintaining effective salt rejection. Holey graphene oxide (HGO) nanosheets synthesized by chemical etching using hydrogen peroxide by depressing porous support by vacuum filtration and reduction through contact with hydriodic acid solutions to create r-HGO membranes. Formation of nanopores improves water permeance from 0.4 to 6.6 LM^2/h/bar and with a Na_2SO_4 rejection rate of 98.5%. More importantly, water permeance and Na_2SO_4 rejection reached the first time to the level of commercial PA-based NF membranes [51].

In another work, the enhanced nanofiltration ability of graphene-based membranes was designed by adding graphene oxide nanoribbons (GONRs) to the graphene nanochannels. The designed membranes could efficiently filter small molecules with a high rejection rate of >95% for various dyes (methyl red, methyl orange, methylene blue, and rose bengal) with high water permeance 312.8 LM^2/h/bar. The improved nanofiltration was observed due to the electrically charged and expanded nanochannels [52].

The GO membranes in the aqueous solution limit their wastewater treatment in membrane separation applications. The nanocomposite membrane made up of sarium-MOFs and GO nanosheets were synthesized through the filtration of Sm-MOFs dispersions via *in situ* growth. In this work, GO sheets disallowed the adjacent GO layers expanding in

aqueous solutions, undergoes a stable skeleton membrane structure. Sm-MOFs' addition helps in the enlargement of composite membrane space, which would favorable for higher permeance. On the other hand, the designed composite membranes showed high permeance of 26 LM^2/h/bar indicating three times superior to pristine GO membrane; >91% high rejection rate for RhB and methylene blue dyes proved with long term stability performances [53].

Generally, poor chlorine resistance reduces the service life of the PA membrane in RO. In this work, N-GOQDs were grafted and integrated on the PA membrane surface. Usually, grafting investigations reduces water flux. However, in this work, the flux of the grafted membrane showed enhanced performance compared with commercial bare membranes. The grafted membrane with concentrations of 0.002 mg/ml showed better desalination of water flux of 40 LM^2/h/bar and NaCl rejection of 96.2% compared to bare membrane 36 LM^2/h/bar with 94% rejection rate [54].

Yang et al. developed a GO/AgNPs nanocomposites membrane prepared to determine the side effects of AgNPs for nanofiltration performances. Different AgNPs sizes such as 8, 20, and 33 nm were coated on GO membranes, and the filtration process was evaluated on dead-end filtration mode. Among different sized AgNPs, only 20 nm AgNPs coated GO membranes showed the highest water flux of 106 LM^2/h/bar and 97.73% rejection rate for RhB dye molecules. The mechanism involved in nanofiltration is interlaying spacing and defect size of designed GO/AgNPs membranes [55].

The swelling of GO membranes is one of the disadvantages of liquid separation applications. To avoid this, cross-linking is commonly used to stabilize GO membranes and helps in the enlargement of d-spacing. The hybrid GO/boron nitride membrane is formed through physical and chemical bond formations. Changing the GO nanosheets and amino-modified boron nitride facilitates plane-plane confirmation, edge–edge covalent bonding, which helps develop compactly packed laminar structure, preventing membrane swelling. Further, the designed stable membrane was able to show 99.98% of rejection rate and 4.15 LM^2/h/bar of flux performances for methylene blue target pollutant [56].

It is important to note that most GO laminar membranes have poor water flux and high rejections for both dyes and salts, which is usually not recommended for dye/salt separations. In this work, NH_2-Fe_3O_4 was introduced on GO nanosheets through vacuum filtration method. The advantages of NH_2-Fe_3O_4 act as a rigid spherical nanospacer to fine-tune GO interlayer spacing and cross-linkers to enhance the stability of GO membranes. The 8 wt% loading of NH_2-Fe_3O_4 exhibited improved water flux of 78 LM^2/h/bar, which is 4.8 superior to pristine GO membrane. Also, it showed 94% of congo red rejection rate and low NaCl rejection performances suggesting effective dye/salt mixture separation [57].

Wu et al. fabricated glycine mediated GO/g-C_3N_4 lamellar membranes for nanofiltration. In this work, glycine acts as a linker for the improved interactions among GO and g-C_3N_4. Also, g-C_3N_4 and glycine help to increase the interlayer spacing of GO membranes. When compared to bare GO membranes, composite membranes showed rapid water transportations. Furthermore, surface modifications by introducing hyperbranched polyethyleneimine (HPEI) coating showed excellent separation performances. The developed membranes showed rejection rates for RhB 77.7, Alcian blue (AB) 89.5, Eosin Y (EY) 91, Evas blue (EB) 99.4%, respectively, with permeance of 15.7 and 42.9 LM^2/h/bar [58].

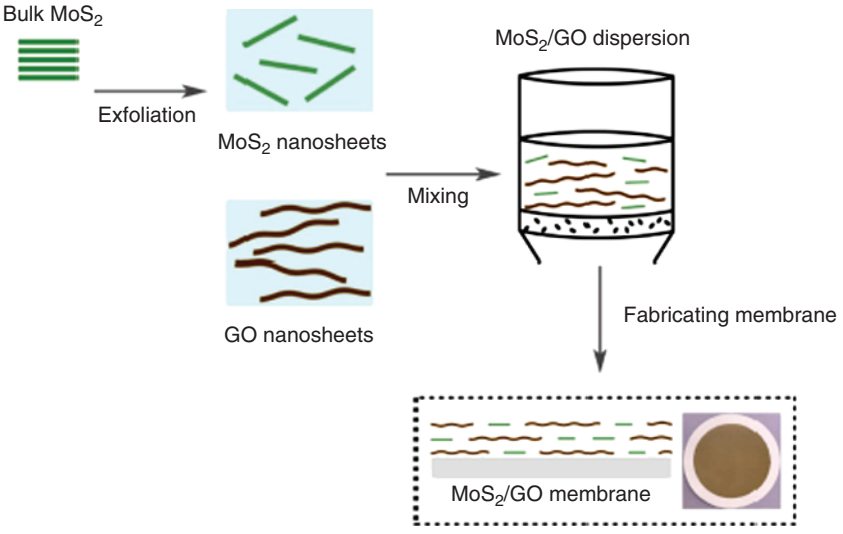

Figure 1.17 Fabrication of MoS_2/GO nanocomposite membrane. Source: Ma et al. [59]. © 2020 Elsevier.

A facile method was established to decrease the repulsive hydration among GO sheets by intercalating MoS_2 on GO nanosheets, and their fabrication process is shown in Figure 1.17. The strong van der Waals forces among MoS_2 and GO, weak interactions between MoS_2 and water molecules and swelling of GO membranes were prominently reduced. The smooth surface of MoS_2 provides with high water flux of 48 LM^2/h/bar. Additionally, separation performance with rejection rates for various dyes 99.99%, 99.90%, 99.76%, 99.66% for DR80, CR, RhB, and MB dyes. Also, rejection rates for various salts 96.85% $K_3Fe(CN)_6$, 66.76% Na_2SO_4, 58.31% $MgSO_4$, 56.00% NaCl, and 44.85% for $MgCl_2$ was observed [59].

In another work, solvothermal induced 2D rGO-TiO_2 with laminar structure was constructed as building blocks for the enhanced separation permeance. The specific properties of designed rGO-TiO_2 membranes such as high surface area, interfacial effects, and narrow layer spacing for size exclusion showed >97% rejection rates for various dye molecules RhB, methyl orange, methylene blue, and congo red. Also, it attained good permeance of 9.36 LM^2/h/bar under the cross-flow filtration process [60].

The graphene oxide nanomembranes (GONMs) with different reduction degrees from diverse graphitic resources proved for water purification performances. The main differences in various functionalities present on the GO surfaces such as (carboxyl (–COOH) or C-GO, hydroxyl (–OH) or H-GO, and epoxy (–COC) or E-GO which is not clearly understood the role of oxygen-bearing groups in the purification process. Thus, in this report, a systematic study was performed on C-GO, H-GO, and E-GO among three oxygen-bearing functional groups. To know the surface properties (Zeta analysis) and d-spacing (XRD) was performed. The obtained results showed oxygen functional groups with diverse hydrophilicity and electricity changed the d-spacing of GONMs and C-GONMs with more negative

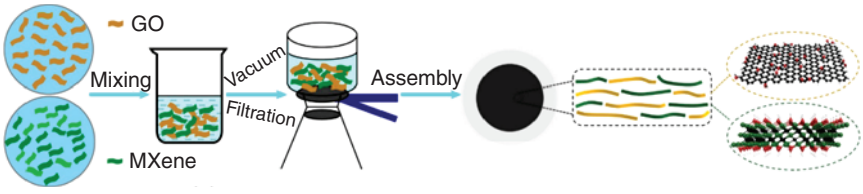

Figure 1.18 Fabrication and assembly of GO/MXene via vacuum filtration process. Source: Liu [62]. © 2020 Elsevier.

charges showed best performances >99% of rejection rate for Trypan blue (TB) dye due to electrostatic effects [61].

In this work, a novel composite membrane based on GO and MXene is demonstrated, and fabrication strategies are represented in Figure 1.18. The important heterogeneous structure of GO/MXene membranes with a different synergistic effect in substrate rejection and permeability was observed. The designed GO/MXene based membranes showed a higher water flux of 71.9 LM^2/h/bar than the pristine GO membrane showed only 6.5 LM^2/h/bar. The rejection of various organic dye molecules such as neutral red (NR), methylene blue (MB), crystal violet (CV), and brilliant blue (BB) exhibited >99.5% efficiencies indicating effective membranes in water treatment [62].

A hierarchical carbon membrane (HCM) was fabricated through a successive vacuum filtration of carbon fiber (CF) substrate, a CNT intermediate supportive layer, and a GO layered membrane. Fabricated HCM membranes were evaluated by capillary flow porometry, thermogravimetric analysis, and membrane performance evaluation. HCM membranes showed an 85% rejection rate for sulfate ions and 1.3 LM^2/h/bar of permeability [63].

In this report, hydrophobic nanofibrous composites for vacuum membrane distillation (VMD) comprising of hydrophobic PVDF nanofibrous layer and hydrophobic polypropylene (PP) nonwoven fabric (NWF) substrate were prepared. The PVDF nanofibrous layer was directly fabricated on the surface of the PP NWF substrate through the electrospinning method. 1*H*, 1*H*, 2*H*, 2*H*-perfluorooctyltriethoxysilane (FTES) modified GO nanosheets were integrated with the PVDF nanofiber layer electrospinning process to improve the hydrophobicity and water flux in VMD. For the designed membranes, the water flux was 36.4 LM^2/h/bar, and NaCl salt rejection was 99.9% [64]. The preparation process and hydrophobic modification of GO nanosheets with FTES are shown in Figure 1.19.

Halakoo and Feng reported surface functionalization of thin-film composite PA membranes for desalination of high salinity water through pervaporation. The surface modification includes treating the PA membrane with chlorine via LBL assembly of positively charged PEI and negatively charged GO. The chlorination treatment improved water permeability, and combining PEI and GO to the chlorine-treated PA membrane helps in enhanced salt rejections. Designed PEI/GO/LBL membranes for the various aqueous salts such as NaCl, Na_2SO_4, $MgSO_4$, and $MgCl_2$ showed water flux of 8 kg/m^2 h with superior slat rejections of >99.9% [65].

In this work, the significance of nanowrinkles in rGOMs for non-selective water and salt transport by fine-tuning 2D nanochannels and nanowrinkles with three reduction methods

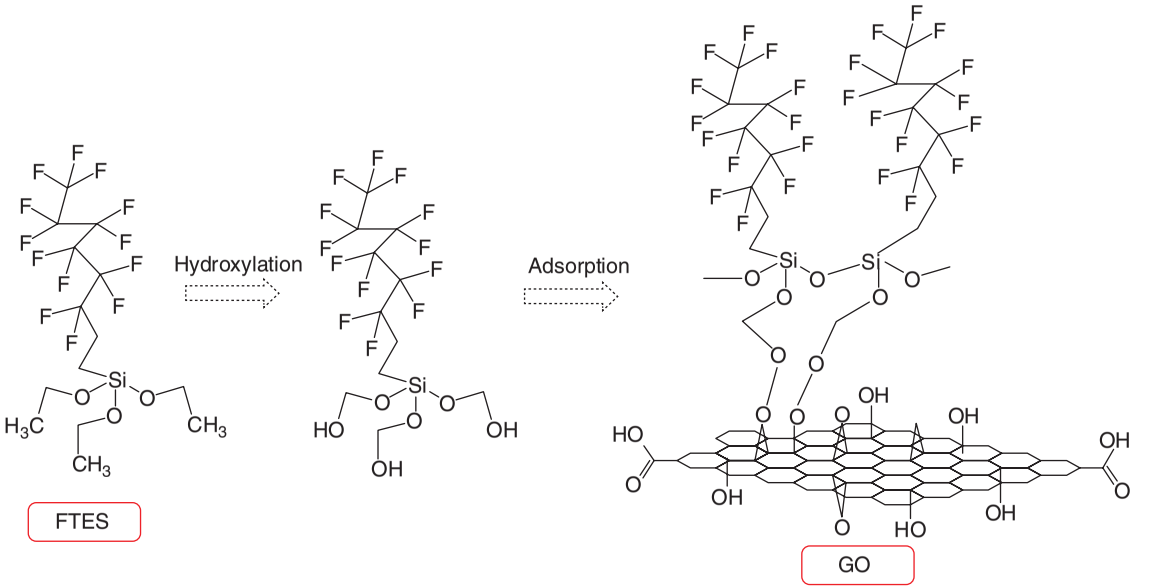

Figure 1.19 Schematic showing a hydrophobic modification of GO nanosheets with FTES. Source: Li et al. [64].

were demonstrated. In the oxidizing atmosphere of air, non-selective nanowrinkles are reduced mild and moderate air thermal reduction process, which is very important for specific water and salt separations. Thus, designed Air-rGO membranes exhibited a high 83% NaCl rejection with enhanced water flux through a hydraulic pressure-driven separation system [66].

In this current work, improving the stability of GO membranes surface was modified by intercalating ionic polymers rich in benzene and cationic imidazolium (or anionic sulfonic) functionalities helps in cross-linking the adjacent nanosheets through non-covalent interactions. The 2D C-GO (imidazolium interactions/cationic) and A-GO (sulfonic interactions/anionic) in the solvated state could preserve their constancy for a longer period. In contrast, solvated GO membranes would instantly decompose when immersed in water. In nanofiltration applications, both 2D C-GO and A-GO showed high permeances of 1111, and 600 LM^2/h/bar under 5 bar compared to pristine GO membrane showed only 65 LM^2/h/bar. Also, in desalination, the 2D C-GO membranes with high water flux of 2.49 LM^2/h/bar and NaCl salt rejection of 95% compared with GO membrane 1.66 LM^2/h/bar and rejection of 76% was observed [67].

GO and rGO significantly used as membranes in water treatment applications. Nevertheless, the main drawbacks are swollen nature and unstable after contact with aqueous solutions. In this work, membranes produced from GO were synthesized using liquid-phase exfoliation, having less oxygen content, unlike the GO/rGO systems used. Its application in ion sieving is reported. Less oxygen content graphene membranes formed from flakes changing size are used to know the effects of flake morphology on ion transport. Especially, reducing flake length and thickness helps improve the number of tortuosity of nanochannels among the layers, resulting in a substantial ion transport reduction. The smaller flakes showed better surface charge due to defects that inhibit chloride mobility permitting for physical sieving and charge repulsions. As designed, graphene membranes showed outstanding Na^+ rejection 97% and water permeance ~10 times higher than those reported GO-based membranes with higher stability with no witnessed swelling [68].

1.3.4 Translation of Graphene Nanomembranes for Real Applications

In this chapter, many modification concepts and applications are reported, proof of concept stage in researcher labs. There are no many examples of their translation to industrial scale, and the main reason is their scalability and competitiveness compared with established and low-cost nanofiltration membranes (https://www.graphene.manchester.ac.uk/learn/applications/membranes). In recent years, there are several successful examples of scalable production of GO membranes fabricated by coating commercial filtering material. One of the most successful and advanced examples of this development comes from Monash University (Professor M. Majumder) group who collaborated with local graphene company Ionic Industries and developed the first scalable GO membrane production in Figure 1.20. The demonstration and production were able to process and manufacture several hundreds of long membranes using this process. This company is currently in the process of applying this technology to clean water production.

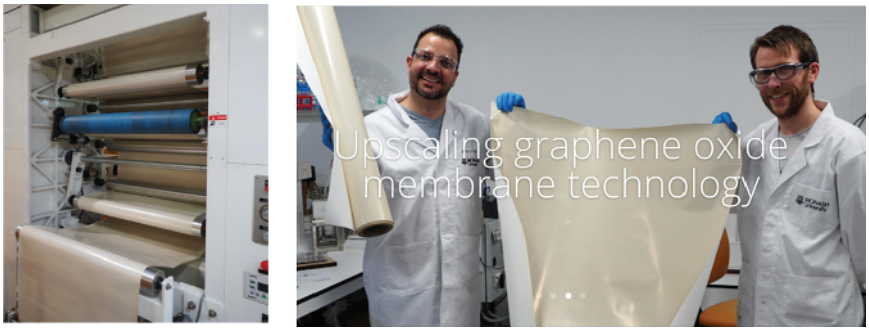

Figure 1.20 Photos showing industrial-scale production of GO membranes in Melbourne, Australia, developed by Monash University and Ionic Industries. Source: https://www.monash.edu/engineering/about-us/news-events/latest-news/articles/2018/monash-pours-enery-into-clean-water-future. Reproduced with permission.

1.4 Graphene Nanomembranes for Heavy Metals Treatment

1.4.1 Heavy Metals

Heavy metallic ions present in the water system are very troublesome to biodegrade. It can easily enter the human body via food chain, instigating a series of irreversible physiological diseases. For example, mercury ions can severely damage the central nervous system, which leads to headaches and gastroenteritis. Lead ions can damage brain tissue, and the excessive amount of lead ions in the body leads to loss of appetite, developmental delay, and hearing impairment. Similarly, other heavy metals have their disadvantages, so it is very important to treat such toxic pollutants safely [69].

An investigation based on the influence of GO nanosheet lateral size on the microstructure and liquid separation performance of ethylene diamine (EDA) cross-linked membranes was studied. Three groups of GO nanosheets with different lateral sizes separated by centrifugation used for membrane preparation in the presence of cross-linker EDA. The designed membrane performed long term stability and exhibited with higher flux rate and >99% of rejection for Cr(VI), showing membrane advantages with constricted d-spacing and enlarged ion size in acidic conditions [70].

The GO and GOMs display excellent rejection for ions, particularly in water treatment. Though, processing and scale-up of GOMs with stability issues persists as one of the major limitations. In this report, fabrication of GOMs with blade casting technique with various cations (K^+, Na^+, Li^+, Mg^{2+}, Ca^{2+}, and Ba^{2+}) intercalation with variable thickness and interlaying spacing. The average water flux obtained for GO-K^+, GO-Ba^{2+} GO-Ca^{2+}, GO-Mg^{2+}, and was 106.35, 46.59, 39.7, and 36.64 LMH. The rejection of Na^+ was 82.57% (GOM-K^+) > 78.6% (GOM-Ba^{2+}) > 75.4% (GOM-Ca^{2+}) > 72.3% (GOM-Mg^{2+}) whereas rejection for Mg^{2+} 98.84% (GOM-K^+) > 97.7% (GOM-Ba^{2+}) > 96.6% (GOM-Ca^{2+}) > 95.57% (GOM-Mg^{2+}). In addition, GOM-Ca^{2+}-R showed highest flux rates and rejection rates for Mg^{2+} (99.5%) followed by Cu^{2+} (98.4%), Ni^{2+} (97%), Pb^{2+} (96%), Na^+ (88.6%) due to the interlayer spacing when associated to other GOMs [71].

Chen et al. reported GO and PES membrane fabricated for separation performance of Hg^{2+} ions, where the GO membrane assembled on PES microfiltration membrane through

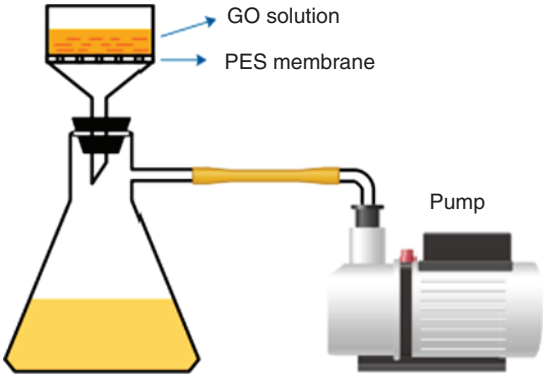

Figure 1.21 GO-PES vacuum-assisted process. Source: Chen et al. [72]. © 2019 American Chemical Society.

vacuum-assisted technique shown in Figure 1.21. The designed GO/PES membranes showed Hg^{2+} retention of 80% and flux of 26.2 LM^2/h bar. Further, the membranes with three circulations maintained the retention rate of 60.63% [72].

In other work, a dual functionalized P_mG_n@PVDF membrane was fabricated by doping GO and followed by PDA coating. The developed membranes showed pure water flux of 188 LMH/h, and Pb^{2+} could remove successfully in the water volume of 2106 LM^2/h/bar. The doping of GO helped maintain Pb^{2+} rejection, which can be ascribed due to the chelation of amino groups present on the PDA layer. Also, actual Pb^{2+} removal was attained to 5029 LM^{-2} due to the addition of citric acid [73].

In this work, TFN FO as a support layer and fabricated in the presence of different concentrations (0–8 wt%) of polyethylene glycol 400, polysulfone, and 1-methyl-2-pyrrolidone through phase inversion process. An active layer is obtained by integrating different weight ratios of (0–0.012 wt%) GO, 1,3-Phenylenediamine, and 1,3,5-benzene trichloride into the PA layer via interfacial polymerization process. The water flux for TFN membrane was 34.3 LMH, enhanced by 174% and 129% compared to TFC membranes 12.5 LMH and commercial FO membrane 15 LMH. Also, the rejection ratios for various metal ions followed the trend lead (99.9%), cadmium (99.7%), and chromium (98.3%) [74].

Harun et al. demonstrated the use of jatropha oil in the fabrication of membrane and their comparison with GO into the polymer matrix. The jatropha oil-based polyol (JOL) was blended with hexamethylene diisocyanate (HDI) to yield jatropha polyurethane membranes (JPU). Further, GO with different loading was prepared to obtain a JPU/GO composite membrane. The water flux enhanced from 223 to 523 LM^2/h. Later, filtration for copper ions showed rejections from 33% to 71.60% [75].

1.5 Conclusion and Future Perspectives

Membrane separation technology authenticated a significant role in wastewater treatments. Many research studies have been focused on separation performances using GO and GO modified/functionalized membranes in water treatment applications in recent years. It has been demonstrated that GO alone and GO modified membranes showed

enhanced membrane properties in terms of mechanical strength, selectivity, flux, rejection, and thermal properties. Various fabrication strategies adapted and reported for GO/GO surface-modified nanomembranes in the desalination process (removal of salts), various dye and heavy metals separation or treatment showed inspiring results. In addition, some of the most promising results paved the information that GO-based nanomembranes could replace some of the existing commercial membranes is demonstrated. Even though several important challenges need to be addressed, such as long-term stability issues and industrial productions, graphene-based nanomembranes are potential low-cost candidates in water treatments. However, the primary key success includes a proper balanced direction toward production costs, and facile manufacturing operations are highly required. Accordingly, it is imperative to advance the expansion of research and development on GO-based nanomembranes. Finally, successful development in GO-based nanomembranes will provide one of the most promising platforms for overcoming the expected global water crisis near future.

Acknowledgments

MDK acknowledges DST, India (DST/BDTD/EAG/2019) and DST Nanomission, India (SR/NM/NS-20/2014) for financial support. DL acknowledges support from ARC Research Hub for Graphene Enabled industry transformation (IH150100003). The authors also thank Jain University, India, for providing facilities.

Important Websites

https://www.google.com/search?q=Graphene+based+nanomembranes+for+sustainable+water+purification+applications&rlz=1C1CHBF_enUS858US858&oq=Graphene+based+nanomembranes+for+sustainable+water+purification+applications&aqs=chrome..69i57.1483j0j7&sourceid=chrome&ie=UTF-8.

https://www.google.com/search?q=Graphene+based+nanomembranes+for+sustainable+water+purification+applications&newwindow=1&rlz=1C1CHBF_enUS858US858&sxsrf=ALeKk03uoBKVyKKhJQH-BtDrCM_2hYmkpA:1603719599866&source=lnms&tbm=isch&sa=X&ved=2ahUKEwjF0MaIsdLsAhWQilwKHcI_AAcQ_AUoAnoECAUQBA&biw=1368&bih=802&dpr=2.

References

1 Du, Y.C., Huang, L.J., Wang, Y.X. et al. (2019). Recent developments in graphene-based polymer composite membranes: preparation, mass transfer mechanism, and applications. *J. Appl. Polym. Sci.* 136: 47761.

2 Lyu, J., Wen, X., Kumar, U. et al. (2018). Separation and purification using GO and r-GO membranes. *RSC Adv.* 8: 23130–23151.

3 Jiang, Y., Biswas, P., and Fortner, J.D. (2016). A review of recent developments in graphene-enabled membranes for water treatment. *Environ. Sci. Water Res. Technol.* 2: 915–922.

4 Boretti, A., Al-Zubaidy, S., Vaclavikova, M. et al. (2018). Outlook for graphene-based desalination membranes. *NPJ Clean Water* 1: 1–11.

5 Kabiri, S., Tran, D.N., Cole, M.A., and Losic, D. (2016). Functionalized three-dimensional (3D) graphene composite for high efficiency removal of mercury. *Environ. Sci. Water Res. Technol.* 2: 390–402.

6 Uthappa, U., Kurkuri, M.D., and Kigga, M. (2019). Nanotechnology advances for the development of various drug carriers. In: *Nanobiotechnology in Bioformulations*, 187–224. Springer.

7 Yap, P.L., Kabiri, S., Tran, D.N., and Losic, D. (2018). Multifunctional binding chemistry on modified graphene composite for selective and highly efficient adsorption of mercury. *ACS Appl. Mater. Interfaces* 11: 6350–6362.

8 Fathizadeh, M., Xu, W.L., Zhou, F. et al. (2017). Graphene oxide: a novel 2-dimensional material in membrane separation for water purification. *Adv. Mater. Interfaces* 4: 1600918.

9 Dervin, S., Dionysiou, D.D., and Pillai, S.C. (2016). 2D nanostructures for water purification: graphene and beyond. *Nanoscale* 8: 15115–15131.

10 Hegab, H.M. and Zou, L. (2015). Graphene oxide-assisted membranes: fabrication and potential applications in desalination and water purification. *J. Membr. Sci.* 484: 95–106.

11 Babu, P., Nambiar, A., He, T. et al. (2018). A review of clathrate hydrate based desalination to strengthen energy–water nexus. *ACS Sustainable Chem. Eng.* 6: 8093–8107.

12 Sriram, G., Uthappa, U., Kigga, M. et al. (2019). Xerogel activated diatoms as an effective hybrid adsorbent for the efficient removal of malachite green. *New J. Chem.* 43: 3810–3820.

13 Song, X., Zambare, R.S., Qi, S. et al. (2017). Charge-gated ion transport through polyelectrolyte intercalated amine reduced graphene oxide membranes. *ACS Appl. Mater. Interfaces* 9: 41482–41495.

14 Zhao, S., Zhu, H., Wang, H. et al. (2019). Free-standing graphene oxide membrane with tunable channels for efficient water pollution control. *J. Hazard. Mater.* 366: 659–668.

15 Wang, X., Wang, H., Wang, Y. et al. (2019). Hydrotalcite/graphene oxide hybrid nanosheets functionalized nanofiltration membrane for desalination. *Desalination* 451: 209–218.

16 Wang, C.-Y., Zeng, W.-J., Jiang, T.-T. et al. (2019). Incorporating attapulgite nanorods into graphene oxide nanofiltration membranes for efficient dyes wastewater treatment. *Sep. Purif. Technol.* 214: 21–30.

17 Fathizadeh, M., Tien, H.N., Khivantsev, K. et al. (2019). Polyamide/nitrogen-doped graphene oxide quantum dots (N-GOQD) thin film nanocomposite reverse osmosis membranes for high flux desalination. *Desalination* 451: 125–132.

18 Cheng, M.-m., L-j, H., Wang, Y.-x. et al. (2019). Reduced graphene oxide–gold nanoparticle membrane for water purification. *Sep. Sci. Technol.* 54: 1079–1085.

19 Ma, J., He, Y., Shi, H. et al. (2019). Stable graphene oxide-based composite membranes intercalated with montmorillonite nanoplatelets for water purification. *J. Mater. Sci.* 54: 2241–2255.

20 Khorramdel, H., Dabiri, E., Tabrizi, F.F., and Galehdari, M. (2019). Synthesis and characterization of graphene acid membrane with ultrafast and selective water transport channels. *Sep. Purif. Technol.* 212: 497–504.

21 Cheng, M.-m., L-j, H., Wang, Y.-x. et al. (2019). Synthesis of graphene oxide/polyacrylamide composite membranes for organic dyes/water separation in water purification. *J. Mater. Sci.* 54: 252–264.

22 Fan, X., Liu, Y., and Quan, X. (2019). A novel reduced graphene oxide/carbon nanotube hollow fiber membrane with high forward osmosis performance. *Desalination* 451: 117–124.

23 Ghaseminezhad, S.M., Barikani, M., and Salehirad, M. (2019). Development of graphene oxide-cellulose acetate nanocomposite reverse osmosis membrane for seawater desalination. *Compos. B. Eng.* 161: 320–327.

24 Kang, H., Wang, W., Shi, J. et al. (2019). Interlamination restrictive effect of carbon nanotubes for graphene oxide forward osmosis membrane via layer by layer assembly. *Appl. Surf. Sci.* 465: 1103–1106.

25 Lee, B., Suh, D.W., Hong, S.P., and Yoon, J. (2019). A surface-modified EDTA-reduced graphene oxide membrane for nanofiltration and anti-biofouling prepared by plasma post-treatment. *Environ. Sci. Nano.* 6: 2292–2298.

26 Luo, Z., Fang, Q., Xu, X. et al. (2019). Attapulgite nanofibers and graphene oxide composite membrane for high-performance molecular separation. *J. Colloid Interface Sci.* 545: 276–281.

27 Fang, S.-Y., Zhang, P., Gong, J.-L. et al. (2020). Construction of highly water-stable metal-organic framework UiO-66 thin-film composite membrane for dyes and antibiotics separation. *Chem. Eng.* 385: 123400.

28 Rajesh, S. and Bose, A.B. (2019). Development of Graphene Oxide Framework Membranes via the "from" and "to" Cross-Linking Approach for Ion-Selective Separations. *ACS Appl. Mater. Interfaces* 11: 27706–27716.

29 Chen, Z., Wang, J., Duan, X. et al. (2019). Facile fabrication of 3D ferrous ion crosslinked graphene oxide hydrogel membranes for excellent water purification. *Environ. Sci. Nano.* 6: 3060–3071.

30 Ou, X., Yang, X., Zheng, J., and Liu, M. (2019). Free-standing graphene oxide–chitin nanocrystal composite membrane for dye adsorption and oil/water separation. *ACS Sustain. Chem. Eng.* 7: 13379–13390.

31 Januário, E.F.D., Beluci, N.C.L., Vidovix, T.B. et al. (2020). Functionalization of membrane surface by layer-by-layer self-assembly method for dyes removal. *Process Saf. Environ. Prot.* 134: 140–148.

32 Xie, A., Cui, J., Yang, J. et al. (2020). Graphene oxide/Fe (III)-based metal-organic framework membrane for enhanced water purification based on synergistic separation and photo-Fenton processes. *Appl. Catal. B.* 264: 118548.

33 Hou, J., Chen, Y., Shi, W. et al. (2020). Graphene oxide/methylene blue composite membrane for dyes separation: Formation mechanism and separation performance. *Appl. Surf. Sci.* 505: 144145.

34 Chang, R., Ma, S., Guo, X. et al. (2019). Hierarchically assembled graphene oxide composite membrane with self-healing and high-efficiency water purification performance. *ACS Appl. Mater. Interfaces* 11: 46251–46260.

35 Fan, X., Cai, C., Gao, J. et al. (2020). Hydrothermal reduced graphene oxide membranes for dyes removing. *Sep. Purif. Technol.* 241: 116730.

36 Li, J., Hu, M., Pei, H. et al. (2020). Improved water permeability and structural stability in a polysulfone-grafted graphene oxide composite membrane used for dye separation. *J. Membr. Sci.* 595: 117547.

37 Zhang, X., Li, H., Wang, J. et al. (2019). In-situ grown covalent organic framework nanosheets on graphene for membrane-based dye/salt separation. *J. Membr. Sci.* 581: 321–330.

38 Gao, Y., Su, K., Wang, X., and Li, Z. (2019). A metal-nano GO frameworks/PPS membrane with super water flux and high dyes interception. *J. Membr. Sci.* 574: 55–64.

39 Khan, N.A., Yuan, J., Wu, H. et al. (2019). Mixed nanosheet membranes assembled from chemically grafted graphene oxide and covalent organic frameworks for ultra-high water flux. *ACS Appl. Mater. Interfaces* 11: 28978–28986.

40 Abadikhah, H., Naderi Kalali, E., Khodi, S. et al. (2019). Multifunctional thin-film nanofiltration membrane incorporated with reduced graphene oxide@TiO_2@Ag nanocomposites for high desalination performance, dye retention, and antibacterial properties. *ACS Appl. Mater. Interfaces* 11: 23535–23545.

41 Zhang, P., Gong, J.-L., Zeng, G.-M. et al. (2019). Novel "loose" GO/MoS_2 composites membranes with enhanced permeability for effective salts and dyes rejection at low pressure. *J. Membr. Sci.* 574: 112–123.

42 Xu, Y., Peng, G., Liao, J. et al. (2020). Preparation of molecular selective GO/$DTiO_2$-PDA-PEI composite nanofiltration membrane for highly pure dye separation. *J. Membr. Sci.* 601: 117727.

43 Yang, Y., Li, Y., Li, Q. et al. (2019). Rapid co-deposition of graphene oxide incorporated metal-phenolic network/piperazine followed by crosslinking for high flux nanofiltration membranes. *J. Membr. Sci.* 588: 117203.

44 Homem, N.C., Beluci, N.d.C.L., Amorim, S. et al. (2019). Surface modification of a polyethersulfone microfiltration membrane with graphene oxide for reactive dyes removal. *Appl. Surf. Sci.* 486: 499–507.

45 Du, Y., Zhang, X., Yang, J. et al. (2020). Ultra-thin graphene oxide films via contra-diffusion method: fast fabrication for ion rejection. *J. Membr. Sci.* 595: 117586.

46 Yu, H., He, Y., Xiao, G. et al. (2020). Weak-reduction graphene oxide membrane for improving water purification performance. *J. Mater. Sci. Technol.* 39: 106–112.

47 Wen, Q., Jia, P., Cao, L. et al. (2020). Electric-field-induced ionic sieving at planar graphene oxide heterojunctions for miniaturized water desalination. *Adv. Mater.*: 1903954.

48 Ambre, J.P., Dhopte, K.B., Nemade, P.R., and Dalvi, V.H. (2019). High flux hyperbranched starch-graphene oxide piperazinamide composite nanofiltration membrane. *J. Environ. Chem. Eng.* 7: 103300.

49 Wang, Q., Zhao, G., Li, C., and Meng, H. (2019). Orderly stacked ultrathin graphene oxide membranes on a macroporous tubular ceramic substrate. *J. Membr. Sci.* 586: 177–184.

50 Wei, Y., Zhu, Y., and Jiang, Y. (2019). Photocatalytic self-cleaning carbon nitride nanotube intercalated reduced graphene oxide membranes for enhanced water purification. *Chem. Eng. J.* 356: 915–925.

51 Chen, X., Feng, Z., Gohil, J. et al. (2019). Reduced holey graphene oxide membranes for desalination with improved water permeance. *ACS Appl. Mater. Interfaces* 12: 1387–1394.

52 Cho, K.M., Lee, H.-J., Nam, Y.T. et al. (2019). Ultrafast-selective nanofiltration of an hybrid membrane comprising laminated reduced graphene oxide/graphene oxide nanoribbons. *ACS Appl. Mater. Interfaces* 11: 27004–27010.

53 Yang, G., Zhang, D., Zhu, G. et al. (2020). A Sm-MOF/GO nanocomposite membrane for efficient organic dye removal from wastewater. *RSC Adv.* 10: 8540–8547.

54 Yi, Z., Shao, F., Yu, L. et al. (2020). Chemical grafting N-GOQD of polyamide reverse osmosis membrane with improved chlorine resistance, water flux and NaCl rejection. *Desalination* 479: 114341.

55 Yang, K., Huang, L.-j., Wang, Y.-x. et al. (2020). Graphene oxide nanofiltration membranes containing silver nanoparticles: tuning separation efficiency via nanoparticle size. *Nanomaterials* 10: 454.

56 Lin, H., Mehra, N., Li, Y., and Zhu, J. (2020). Graphite oxide/boron nitride hybrid membranes: the role of cross-plane laminar bonding for a durable membrane with large water flux and high rejection rate. *J. Membr. Sci.* 593: 117401.

57 Dong, L., Li, M., Zhang, S. et al. (2020). NH_2-Fe_3O_4-regulated graphene oxide membranes with well-defined laminar nanochannels for desalination of dye solutions. *Desalination* 476: 114227.

58 Wu, Z., Gao, L., Wang, J. et al. (2020). Preparation of glycine mediated graphene oxide/g-C_3N_4 lamellar membranes for nanofiltration. *J. Membr. Sci.* 601: 117948.

59 Ma, J., Tang, X., He, Y. et al. (2020). Robust stable MoS_2/GO filtration membrane for effective removal of dyes and salts from water with enhanced permeability. *Desalination* 480: 114328.

60 Yu, J., Zhang, Y., Chen, J. et al. (2020). Solvothermal-induced assembly of 2D-2D rGO-TiO_2 nanocomposite for the construction of nanochannel membrane. *J. Membr. Sci.* 600: 117870.

61 Yu, H., He, Y., Xiao, G. et al. (2020). The roles of oxygen-containing functional groups in modulating water purification performance of graphene oxide-based membrane. *Chem. Eng. J.* 389: 124375.

62 Liu, T., Liu, X., Graham, N. et al. (2020). Two-dimensional MXene incorporated graphene oxide composite membrane with enhanced water purification performance. *J. Membr. Sci.* 593: 117431.

63 Amadei, C.A., Arribas, P., Cruzado, L., and Vecitis, C. (2020). Graphene oxide membranes on a hierarchical elemental carbon-based support. *Environ. Sci.: Nano*.

64 Li, H., Shi, W., Zeng, X. et al. (2020). Improved desalination properties of hydrophobic GO-incorporated PVDF electrospun nanofibrous composites for vacuum membrane distillation. *Sep. Purif. Technol.* 230: 115889.

65 Halakoo, E. and Feng, X. (2020). Layer-by-layer assembly of polyethyleneimine/graphene oxide membranes for desalination of high-salinity water via pervaporation. *Sep. Purif. Technol.* 234: 116077.

66 Yuan, S., Li, Y., Xia, Y. et al. (2020). Minimizing non-selective nanowrinkles of reduced graphene oxide laminar membranes for enhanced NaCl rejection. *Environ. Sci. Technol. Lett.* 7: 273–279.

67 Ran, J., Chu, C., Pan, T. et al. (2019). Non-covalent cross-linking to boost the stability and permeability of graphene-oxide-based membranes. *J. Mater. Chem. A* 7: 8085–8091.

68 Hirunpinyopas, W., Iamprasertkun, P., Bissett, M.A., and Dryfe, R.A. (2020). Tunable charge/size selective ion sieving with ultrahigh water permeance through laminar graphene membranes. *Carbon* 156: 119–129.

69 Wang, Z., Wu, A., Colombi Ciacchi, L. et al. (2018). Recent advances in nanoporous membranes for water purification. *Nanomaterials* 8: 65.

70 Lin, H., Li, Y., and Zhu, J. (2020). Cross-linked GO membranes assembled with GO nanosheets of differently sized lateral dimensions for organic dye and chromium separation. *J. Membr. Sci.* 598: 117789.

71 Ghaffar, A., Zhang, L., Zhu, X., and Chen, B. (2019). Scalable graphene oxide membranes with tunable water channels and stability for ion rejection. *Environ. Sci.: Nano* 6: 904–915.

72 Chen, H., Wu, H., Wang, Q. et al. (2019). Separation performance of Hg^{2+} in desulfurization wastewater by the graphene oxide polyethersulfone membrane. *Energy Fuels* 33: 9241–9248.

73 Zhang, Y., Feng, Y., Xiang, Q. et al. (2020). A high-flux and anti-interference dual-functional membrane for effective removal of Pb(II) from natural water. *J. Hazard. Mater.* 384: 121492.

74 Saeedi-Jurkuyeh, A., Jafari, A.J., Kalantary, R.R., and Esrafili, A. (2020). A novel synthetic thin-film nanocomposite forward osmosis membrane modified by graphene oxide and polyethylene glycol for heavy metals removal from aqueous solutions. *React. Funct. Polym.* 146: 104397.

75 Harun, N.H., Abidin, Z.Z., Abdullah, A.H., and Othaman, R. (2020). Sustainable jatropha oil-based membrane with graphene oxide for potential application in Cu(II) ion removal from aqueous solution. *Processes* 8: 230.